Eur. Phys. J. Special Topics **222**, 487–500 (2013)

DOI: 10.1140/epjst/e2013-01854-7

THE EUROPEAN PHYSICAL JOURNAL SPECIAL TOPICS

Regular Article

# Quantifying heart rate dynamics using different approaches of symbolic dynamics

D. Cysarz[1,a], A. Porta[2], N. Montano[3], P.V. Leeuwen[4], J. Kurths[5,6], and N. Wessel[5]

[1] Integrated Studies for Anthroposophic Medicine; Chair for Theory of Medicine, Integrative and Anthroposophic Medicine, Faculty for Health, University of Witten/Herdecke, Germany
[2] Department of Biomedical Sciences for Health, Galeazzi Orthopedic Institute, University of Milan, Italy
[3] Department of Biomedical and Clinical Sciences, Internal Medicine II, L. Sacco Hospital, University of Milan, Milan, Italy
[4] Department of Radiology and Microtherapy, Faculty for Health, University of Witten/Herdecke, Germany
[5] Cardiovascular Physics, Department of Physics, Humboldt-Universität zu Berlin, Germany
[6] Potsdam Institute for Climate Impact Research, Potsdam, Germany

Received 27 March 2013 / Received in final form 25 April 2013
Published online 25 June 2013

**Abstract.** The analysis of symbolic dynamics applied to physiological time series is able to retrieve information about dynamical properties of the underlying system that cannot be gained with standard methods like e.g. spectral analysis. Different approaches for the transformation of the original time series to the symbolic time series have been proposed. Yet the differences between the approaches are unknown. In this study three different transformation methods are investigated: (1) symbolization according to the deviation from the average time series, (2) symbolization according to several equidistant levels between the minimum and maximum of the time series, (3) binary symbolization of the first derivative of the time series. Furthermore, permutation entropy was used to quantify the symbolic series. Each method was applied to the cardiac interbeat interval series $RR_i$ and its difference $\Delta RR_I$ of 17 healthy subjects obtained during head-up tilt testing. The symbolic dynamics of each method is analyzed by means of the occurrence of short sequences ("words") of length 3. The occurrence of words is grouped according to words without variations of the symbols (0V%), words with one variation (1V%), two like variations (2LV%) and two unlike variations (2UV%). Linear regression analysis showed that for method 1 0V%, 1V%, 2LV% and 2UV% changed with increasing tilt angle. For method 2 0V%, 2LV% and 2UV% changed with increasing tilt angle and method 3 showed changes for 0V% and 1V%. Furthermore, also the permutation entropy decreased with increasing tilt angle. In conclusion, all methods are capable of reflecting changes of the cardiac autonomic nervous system during head-up tilt. All methods show that

[a] e-mail: d.cysarz@rhythmen.de

even the analysis of very short symbolic sequences is capable of tracking changes of the cardiac autonomic regulation during head-up tilt testing.

## 1 Introduction

Physiological time series such as the series of successive cardiac interbeat intervals, i.e. heart beat periods, contain rich information. Different linear and nonlinear approaches have been used to characterize dynamical features. E.g. spectral analysis has been used to quantify the amount of sinus-like oscillations, thus disregarding statistical moments of order higher than two. Low (0.04–0.15 Hz) and high frequency (0.15–0.4 Hz) oscillations have then been linked to the modulations of both branches of the autonomic nervous system (ANS) [1–3].

Dynamical aspects of physiological time series may be analyzed by means of symbolic dynamics. Different approaches have been developed and applied to physiological time series. One approach to symbolize the times series is based on the amount of deviation from the average heart rate (or, equivalently, average interbeat interval) [4,5]. The complexity of the resulting symbolic patterns has been quantified using Shannon or Renyi entropy [5]. Furthermore, the amount of occurrence (or non-occurrence, i.e. 'forbidden words') of symbolic patterns complements information retrieved from spectral analysis in patients threatened by sudden cardiac death [6]. This symbolization approach has also been extended to quantify time-delayed couplings between e.g. heart rate and blood pressure modulations [7] or to quantify cardiorespiratory interaction [8].

Another approach spans the interval between the minimum and the maximum of the time series over a fixed amount of symbols [9]. This interval is divided into several equidistant steps. The resulting symbolic patterns were classified according to the amount of variations in the patterns. The amount of occurrence of patterns with 0, 1 or 2 variations also complements the information from spectral analysis of a cardiac interbeat interval series [10,11]. The analysis of symbolic patterns during graded head-up tilt showed that the occurrence of specific symbolic patterns is linked to sympathetic and parasympathetic modulations of the ANS [11].

A third approach uses only two symbols and is used in two different ways. One method symbolizes the succession of acceleration and deceleration of the instantaneous heart rate [12,13]. Using this method it has been shown that the interbeat interval series from healthy subjects contains a large amount of regular binary patterns, i.e. patterns with a low number of changes between 0s and 1s [14]. These patterns are also capable of reflecting changes of the cardiac autonomic regulation during head-up tilt [15,16]. The occurrence of regular binary patterns is linked to sympathetic modulations whereas the occurrence of irregular binary patterns is linked to parasympathetic modulations. Furthermore, runs of heart rate decelerations, i.e. symbolic sequences containing only the symbol for deceleration, may be used for the prediction of high risk patients after myocardial infarction [17]. The other method distinguishes between small and large differences between successive interbeat intervals using two symbols [5]. It has been shown that this approach is able to detect differences in heart rate dynamics before the onset of ventricular tachycardia [18] or during different stages of general anesthesia [19]. Both methods retain relevant dynamical properties although a considerable amount of information is disregarded.

Each approach to symbolize the interbeat interval series retrieves specific information that cannot be gained with standard methods like e.g. spectral analysis. However, it is unclear if the approaches deliver different information. In this study is the application of three different approaches of symbolizing the cardiac interbeat interval

series to data obtained during head-up tilt. The first two approaches were applied to the time series as well as the first variations to complement the third approach.

## 2 Methods

### 2.1 Construction of symbolic sequences

In the following three different approaches to transform a time series into a symbolic series are presented. The approaches are presented for the general case of a time series $x_i$.

#### 2.1.1 $\sigma$-method

The time series $x_i$ is transformed into the symbol sequence $S_{\sigma,i}$ $(i = 1, \ldots, N)$ using the alphabet $A = \{0, 1, 2, 3\}$ as follows [5]:

$$S_{\sigma,i} = \begin{cases} 0 & : & \mu & < x_i \leq (1+a)\cdot\mu \\ 1 & : & (1+a)\cdot\mu & < x_i < \infty \\ 2 & : & (1-a)\cdot\mu & < x_i \leq \mu \\ 3 & : & 0 & < x_i \leq (1-a)\cdot\mu \end{cases} \tag{1}$$

This transformation transforms the time series according to the deviation from the average of $x_i$. The transformation uses three different quantization levels: $\mu$ denotes the average $x_i$, $(1+a)\cdot\mu$ and $(1-a)\cdot\mu$ are thresholds above respectively below the average according to the parameter $a$. In this study $a$ is set to 0.05, i.e. the upper and lower threshold are 5% above respectively below the average. This choice has proven to yield reliable results if applied to the cardiac interbeat interval time series [5].

#### 2.1.2 Max-min-method

To obtain a symbolic time series $S_{max-min,i}$ that comprises the full range of dynamics of the time series $x_i$ the difference between the minimum and the maximum of $x_i$ is divided into a $\xi$ quantization bins of size $l = (\max(x_i) - \min(x_i))/\xi$. Hence, this transformation has the alphabet $A = \{0, 1, \ldots, \xi - 1\}$ [11]. The transformation is as follows:

$$S_{max-min,i} = \begin{cases} 0 & : & \min(x_i) & \leq x_i < 1\cdot l \\ 1 & : & 1\cdot l & \leq x_i < 2\cdot l \\ & & \vdots & \\ \xi-1 & : & (\xi-1)\cdot l & \leq x_i \leq \max(x_i), \end{cases} \tag{2}$$

The number of quantization levels is set to $\xi = 6$ and the sequence length is set to $k = 3$. This is a good compromise for short time series [11].

This definition is also applied to the interbeat interval series $RR_i$, $i = 1, \ldots, N$ (absolute values) and to the differences between successive interbeat intervals $\Delta RR_i = RR_i - RR_{i-1}$, $i = 2, \ldots, N$.

#### 2.1.3 Binary $\Delta$-coding-method

In difference to the two former methods this transformation makes use of differences between successive elements of the time series $x_i$ instead of taking the absolute values

of the time series. A binary series $S_{bin\Delta,i}$ $(i = 1, \ldots, N-1)$ was created using the differences $\Delta x_i = x_i - x_{i-1}$, $(i = 2, \ldots, N)$ using a binary alphabet $A = \{0, 1\}$ [12]:

$$S_{bin\Delta,i} = \begin{cases} 0 & : \quad \Delta x_{i+1} \geq 0 \\ 1 & : \quad \Delta x_{i+1} < 0 \end{cases} \tag{3}$$

$\Delta RR_i = RR_i - RR_{i-1}$, $i = 2, \ldots, N$ is used as the time series $\Delta x_i$. Hence, in this definition the "decelerations" of the interbeat intervals are symbolized by 0s, "accelerations" by 1s.

A variation of this method is used for binary coding if the symbolization is to reflect small and large differences between successive interbeat intervals [5]:

$$S_{bin\Delta,\tau,i} = \begin{cases} 0 & : \quad |\Delta x_{i+1}| < \tau \\ 1 & : \quad |\Delta x_{i+1}| \geq \tau \end{cases} \tag{4}$$

Like in other studies $\tau = 10$ ms is used as threshold between small and large differences between successive interbeat intervals [18,19]. Note that the absolute values of $\Delta x_{i+1}$ are used in this definition.

## 2.2 Analysis of symbolic dynamics

### 2.2.1 Variations within symbolic sequences ("words")

The dynamics of the symbolic series $S_i$ is analyzed using symbolic sequences of length $k$ (also referred to as "words"). I.e. symbolic sequences are constructed using delayed coordinates as $w_i = (S_i, S_{i+1}, \ldots, S_{i+k-1})$, $i = 1, \ldots, N-k+1$. In this study symbolic sequences of length $k = 3$ are analyzed.

The sequences of length $k$ are categorized according to their amount of variations between successive symbols as follows [11]:

- No variation between successive symbols (0V sequences)
- One variation between successive symbols (1V sequences)
- Two like variations between successive symbols (2LV sequences). I.e. two successive increases or decreases (e.g. "321" or "123").
- Two unlike variations between successive symbols (2UV sequences). I.e. one decrease followed by an increase or vice versa.

This categorization can only be applied to the symbolic series $S_{\sigma,i}$ and $S_{max-min,i}$ because the binary symbolic series $S_{bin\Delta,i}$ and $S_{bin\Delta,\tau,i}$ cannot differentiate between "two like variations" and "two unlike variations" (see below). For $S_{\sigma,i}$ this categorization of the $4^3 = 64$ different sequences results in four 0V sequences, 24 1V sequences, 8 2LV sequences and 28 2UV sequences. The percent occurrence of these patterns were designated 0V%, 1V%, 2LV% and 2UV%. For example, 0V% was calculated as (No. of occurrence of 0V sequences)$/(N-2) \cdot 100$ and likewise for the other categories. For $S_{max-min,i}$ the categorization of the $6^3 = 216$ different sequences results in six 0V sequences, 60 1V sequences, 40 2LV sequences and 110 2UV sequences. The percent occurrence of these patterns were designated 0V%, 1V%, 2LV% and 2UV%.

$S_{\sigma,i}$ and $S_{max-min,i}$ can be created using the interbeat interval series $RR_i$, $i = 1, \ldots, N$ (absolute values) and the differences between successive interbeat intervals $\Delta RR_i = RR_i - RR_{i-1}$, $i = 2, \ldots, N$. Hence, an appropriate subscript is added to the mentioned quantities to distinguish them with respect to the original series (e.g. $0V\%_a$: 0V% for *a*bsolute values $RR_i$; $0V\%_d$: 0V% for *d*ifferences $\Delta RR_i$).

The binary sequences $S_{bin\Delta,i}$ and $S_{bin\Delta,\tau,i}$ can be categorized in a similar fashion. Again, binary sequences of length $k = 3$ are analyzed. The classification of the $2^3 = 8$ different sequences is analogously to the above mentioned categorization. E.g. the sequence "000" has no variation whereas e.g. "001" has one variation and "010" has two variations ($0 \to 1$ and $1 \to 0$). Using this scheme the maximum amount of variations for binary patterns of length $k$ is $k - 1$. Hence, $k = 3$ results in a categorization of binary sequences in analogy to the other two symbolizations approaches: no variation: 0V (two binary sequences), one variation: 1V (four binary sequences), two variations: 2V (two binary sequences). The rate occurrence of these patterns were designated 0V%, 1V% and 2V%.

#### 2.2.2 Calculation of permutation entropy

Permutation entropy was introduced as a complexity measure for time series [20]. The symbolic series $S_i$ is analyzed with respect to symbolic sequences $w_i$ of length $k$. Each sequence $w_i$ is sorted in ascending order (e.g. $(3, 4, 1) \to (1, 3, 4)$) and the permutation $\pi$ necessary for this sort is counted for each occurrence: $n(\pi) = \#\{i | i = 1, \ldots, N - k + 1; w_i \text{ has type } \pi\}$. The relative occurrence is $p(\pi) = n(\pi)/(N - k + 1)$. The permutation entropy of order $n$ is defined as:

$$H(n) = -\sum_{1}^{n!} p(\pi) \log_2 p(\pi). \tag{5}$$

Note that the logarithm is calculated to the base 2 and, hence, $H(n)$ is expressed in bits. In this study, the permutation entropy $H(n)$ is calculated for $n = 3$ in analogy to the categorization of the variations within symbolic sequences. $H(n)$ is calculated for the symbolic series $S_{\sigma,i}$ and $S_{max-min,i}$ using the interbeat interval series $RR_i$ (permutation entropies $H_{\sigma,RR}$ and $H_{max-min,RR}$) and the differences between successive interbeat intervals $\Delta RR_i$ (permutation entropies $H_{\sigma,\Delta RR}$ and $H_{max-min,\Delta RR}$). Furthermore $H(n)$ was calculated for the binary sequences $S_{bin\Delta,i}$ and $S_{bin\Delta,\tau,i}$ (permutation entropies $H_{bin\Delta,i}$ and $H_{bin\Delta,\tau,i}$).

### 2.3 Experimental protocol

17 out of 18 healthy subjects (non-smoker, median age: 28 years, age range 21–54 years, 7 women) were enrolled in the study at the University of Milan [11]. One subject felt uncomfortable during the session with tilt table inclination of 75° and, hence, this subject was excluded from the analysis. The subjects did not take any medication, nor did they consume any caffeine- or alcohol-containing beverages in 24 h before the recording. While the subjects were on the tilt table, they were supported by two belts at the level of the thigh and the waist. Both feet touched the footrest of the tilt table. The subjects breathed spontaneously but were not allowed to talk during the protocol. The study complies to the principles of the Declaration of Helsinki and has been approved by the review board of the L. Sacco Hospital, University of Milan.

ECG (lead II) was recorded during the procedure at a sampling rate of 1000 Hz. After 7 minutes at rest, the subject were subjected to 10 min of tilt with table angles randomly chosen within the set {15°, 30°, 45°, 60°, 75°, and 90°}. Each tilt session was preceded by a rest period and followed by 3 minutes of recovery. All enrolled subjects were able to complete the overall sequence of tilt table inclinations without a sign of pre-syncope.

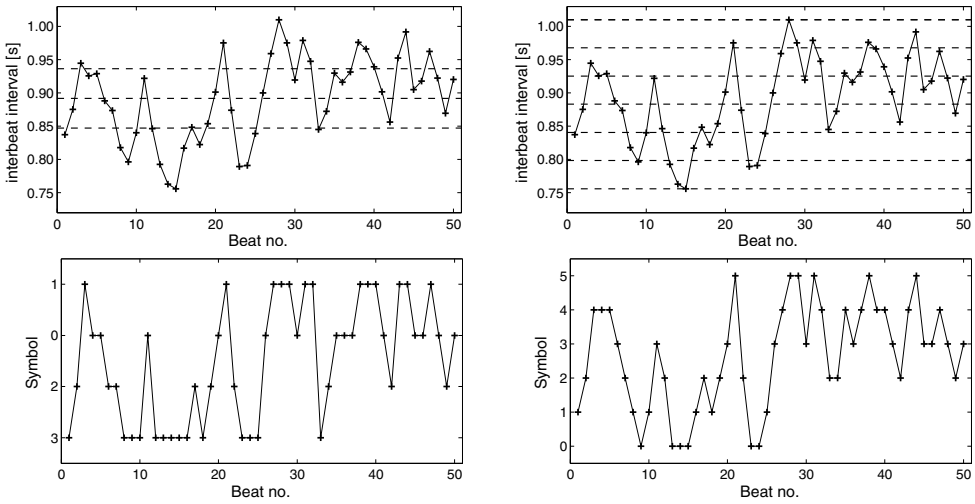


**Fig. 1.** Examples of $\sigma$-method and Max-min-method. Top left: Transformation based on average interbeat interval (middle dashed line), average+5% (upper dashed line) and average-5% (lower dashed line). Top right: Transformation based on maximum and minimum interbeat interval and six quantization levels (see dashed lines). Lower diagrams show resulting symbolic series.

### 2.4 Data extraction

After the QRS complex was detected on the ECG and the apex of the R wave was located using parabolic interpolation, the heart period was automatically calculated on a beat-to-beat basis as the time between two consecutive R peaks (RR interval). All QRS determinations were carefully checked to avoid erroneous detections or missed beats. The length $N$ of the series $RR_i$ ranged from 220 to 260 beats and was kept constant while the experimental condition was varied in the same subject. The average $RR_i$ and its accompanying standard deviation served as basic parameters to reflect changes of the cardiac autonomic regulation during head-up tilt.

### 2.5 Statistical analysis

Linear regression analysis between all the parameters and tilt angles was carried out using Spearman rank-order correlation. Global linear regression (GLR) was calculated using pooled data from all subjects. For individual linear regression (ILR) analysis, only one subject was considered at a time. ILR analysis was carried out only if global linear regression analysis was significant; in this case, we calculated the percentage of subjects with a significant ILR analysis (ILR%). $P < 0.05$ was considered significant.

## 3 Results

An example illustrating the different approaches to symbolic dynamics is shown in Figs. 1 ($\sigma$- and Max-min-method) and 2 (Binary $\Delta$-coding-methods). A qualitative comparison between the two symbolic series in Fig. 1 ($\sigma$-method and max-min-method) shows that both methods resemble dynamical aspects of the original

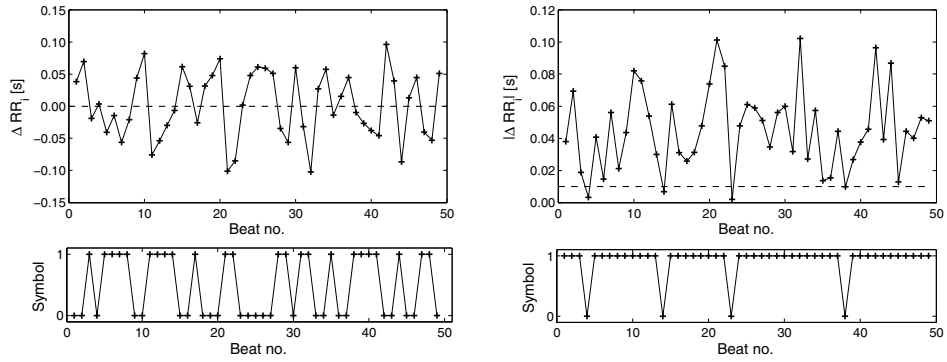


**Fig. 2.** Examples of Binary Δ-coding-method. Left column: transformation based on acceleration ($\Delta RR_i < 0$, 1s) and deceleration ($\Delta RR_i \geq 0$, 0s) of successive interbeat intervals. Right column: transformation based on small (0s) and large differences (1s) between successive interbeat intervals (dashed line: threshold). The lower diagrams show the resulting binary series.

**Table 1.** Average $RR_i$ and its accompanying standard deviation (SD). Values are expressed as median (1st quartile–3rd quartile).

| | 0° | 15° | 30° | 45° | 60° | 75° | 90° |
|---|---|---|---|---|---|---|---|
| RR [ms] | 974 | 905 | 827 | 791 | 749 | 744 | 728 |
| | 912–1044 | 813–1053 | 777–896 | 723–868 | 656–816 | 654–786 | 668–803 |
| SD(RR) [ms] | 61 | 64 | 53 | 53 | 50 | 45 | 48 |
| | 45–76 | 43–78 | 42–65 | 36–59 | 31–72 | 32–61 | 29–65 |

time series. It is evident that the more quantization levels used for the transformation the more detailed the dynamical aspects. The binary representation (Fig. 2) delivers different information because it is not based on the absolute values of the interbeat interval series but on the series of differences between successive interbeat intervals. The series $S_{bin\Delta,i}$ represents each change of the sign of $\Delta RR$, i.e. the changes between acceleration and deceleration of the heart rate. It is evident that the series $S_{bin\Delta,10,i}$ shows a more regular binary series, i.e. longer successions of successive 0s and 1s, because it distinguishes between small and large variations of $|\Delta RR_i|$ and this example mostly contains large variations.

During the head-up tilt test the average interbeat interval $RR_i$ progressively decreases with increasing tilt angle, i.e. the heart rate increases (see Table 1). The accompanying standard deviation also decreases with increasing tilt angle. However, the decrease is less uniformly spread, i.e. a clear decrease can only be found between 15° and 30° and also between 60° and 75°.

### 3.1 Variations within symbolic sequences

For the symbolic sequences derived from $RR_i$ the occurrence of the 0V, 1V, 2LV and 2UV sequences (i.e. $0V\%_a$, $1V\%_a$, $2LV\%_a$ and $2UV\%_a$) with increasing tilt angle are shown in Table 2 and Fig. 3. For the $\sigma$-method the symbolic sequence $0V\%_a$ increases progressively up to a tilt angle of 60°. $1V\%_a$ progressively decreases only at tilt angles 30° to 60°. $2LV\%_a$ and $2UV\%_a$ show a progressive decrease up to a tilt angle of 60°. With respect to the Min-max-method the following results were obtained. Similar to the aforementioned results $0V\%_a$ increases progressively up to a tilt angle of 60°.

**Table 2.** Symbolic indexes during graded head-up tilt calculated from the symbolic series $S_i$ (constructed using $RR_i$). Values are expressed as median (1st quartile–3rd quartile).

| Index | 0° | 15° | 30° | 45° | 60° | 75° | 90° |
|---|---|---|---|---|---|---|---|
| $\sigma$-method | | | | | | | |
| 0V%$_a$ | 17.2 | 25.1 | 38.2 | 42.8 | 50.6 | 48.0 | 49.4 |
| | 12.5–24.7 | 21.2–36.6 | 29.7–42.2 | 38.2–47.3 | 44.9–59.1 | 43.1–56.2 | 44.1–56.7 |
| 1V%$_a$ | 46.7 | 45.2 | 47.0 | 43.4 | 37.1 | 38.2 | 39.7 |
| | 41.6–51.2 | 41.5–50.7 | 40.1–48.1 | 39.7–45.9 | 34.5–43.4 | 36.0–45.8 | 34.7–44.9 |
| 2LV%$_a$ | 13.5 | 11.6 | 8.7 | 7.2 | 6.2 | 6.3 | 5.9 |
| | 8.6–18.3 | 8.5–14.1 | 5.4–12.7 | 2.0–11.0 | 2.7–8.8 | 1.3–8.3 | 2.7-10.0 |
| 2UV%$_a$ | 22.5 | 12.6 | 7.2 | 6.0 | 3.1 | 3.7 | 4.0 |
| | 10.9–27.0 | 7.6–20.6 | 6.3–11.9 | 3.7–9.7 | 1.5–7.2 | 2.4–5.9 | 2.3–7.6 |
| Max-min | | | | | | | |
| 0V%$_a$ | 11.6 | 21.3 | 22.9 | 33.1 | 39.7 | 41.0 | 39.7 |
| | 8.9–14.3 | 12.8–22.2 | 18.7–33.3 | 27.5–41.7 | 31.6–46.1 | 34.6–45.5 | 35.0–45.8 |
| 1V%$_a$ | 46.7 | 49.2 | 48.7 | 46.4 | 45.5 | 45.1 | 45.6 |
| | 42.6–49.3 | 45.9–51.5 | 46.7–52.0 | 45.3–50.4 | 42.2–50.7 | 42.4–49.5 | 42.8–48.8 |
| 2LV%$_a$ | 17.5 | 15.5 | 12.5 | 8.7 | 7.0 | 6.9 | 7.5 |
| | 14.3–21.7 | 13.8–17.9 | 9.0–17.1 | 7.9–11.2 | 5.2–10.5 | 5.5–13.1 | 5.0–11.6 |
| 2UV%$_a$ | 23.8 | 12.6 | 10.4 | 8.0 | 4.0 | 4.5 | 5.2 |
| | 16.5–28.7 | 9.8–21.9 | 6.4–14.6 | 5.2–13.1 | 3.5–10.0 | 3.3–6.2 | 3.1–10.5 |

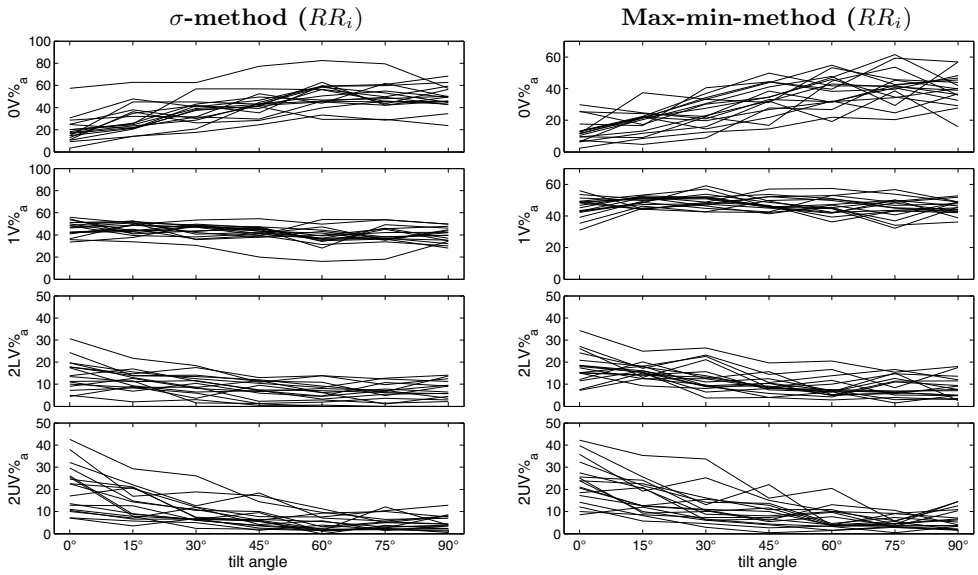


**Fig. 3.** Occurrence of symbolic sequences generated from the $RR_i$ series categorized according to the variation 0V%$_a$, 1V%$_a$, 2LV%$_a$ and 2UV%$_a$ vs. tilt angle. Left column: $\sigma$-method, right column: Max-min-method.

2LV%$_a$ and 2UV%$_a$ decrease progressively in the same range of tilt angles. 1V%$_a$ is constant for all tilt angles.

Using the differences $\Delta RR_i$ to construct the symbolic series $S_i$ shows the following results (cf. Table 3 and Fig. 4). For the $\sigma$-method the symbolic sequence 0V%$_d$ increases progressively over the whole range of tilt angles. At the same time 1V%$_d$ progressively decreases. 2LV%$_d$ is 0 in almost any case except three occurrences with 2LV%$_d$ $< 0.5\%$ (cf. Fig. 5). I.e. the accompanying symbolic sequences do not occur

**Table 3.** Symbolic indexes during graded head-up tilt calculated from the symbolic series $S_i$ (constructed using $\Delta RR_i$). Values are expressed as median (1st quartile–3rd quartile).

| Index | 0° | 15° | 30° | 45° | 60° | 75° | 90° |
|---|---|---|---|---|---|---|---|
| $\sigma$-method | | | | | | | |
| $0V\%_d$ | 12.1 | 23.0 | 30.2 | 36.8 | 38.5 | 42.6 | 45.2 |
| | 9.5–22.2 | 17.5–30.8 | 25.4–36.3 | 26.2–44.8 | 30.7–48.7 | 36.4–50.0 | 30.4–55.8 |
| $1V\%_d$ | 66.2 | 63.1 | 59.6 | 51.5 | 44.8 | 45.3 | 41.8 |
| | 61.0–74.2 | 57.4–70.2 | 51.0–66.1 | 46.1–65.8 | 42.3–55.4 | 39.0–49.9 | 36.3–54.0 |
| $2LV\%_d$ | 0.0 | 0.0 | 0.0 | 0.0 | 0.0 | 0.0 | 0.0 |
| | 0.0–0.0 | 0.0–0.0 | 0.0–0.0 | 0.0–0.0 | 0.0–0.0 | 0.0–0.0 | 0.0–0.0 |
| $2UV\%_d$ | 11.0 | 11.2 | 9.7 | 10.5 | 12.6 | 10.1 | 11.1 |
| | 8.6–23.7 | 8.4–14.6 | 5.8–16.0 | 6.7–15.6 | 4.7–17.1 | 7.9–17.3 | 6.1–16.0 |
| Max-min | | | | | | | |
| $0V\%_d$ | 4.5 | 7.6 | 9.3 | 11.8 | 15.5 | 21.1 | 17.1 |
| | 2.8–8.1 | 3.1–12.2 | 5.8–16.0 | 8.6–18.9 | 9.6–31.1 | 12.4–34.9 | 12.9–36.1 |
| $1V\%_d$ | 40.3 | 42.9 | 43.5 | 45.5 | 44.5 | 42.2 | 43.4 |
| | 34.4–45.0 | 36.4–45.1 | 37.4–47.7 | 40.4–48.2 | 37.3–48.2 | 40.1–45.9 | 39.8–46.7 |
| $2LV\%_d$ | 21.2 | 22.1 | 17.4 | 15.3 | 10.1 | 10.3 | 8.9 |
| | 13.4–25.5 | 14.9–23.8 | 13.6–24.3 | 11.9–19.1 | 6.7–14.8 | 7.7–15.4 | 6.6–12.9 |
| $2UV\%_d$ | 32.3 | 29.0 | 27.8 | 25.4 | 23.6 | 20.7 | 23.1 |
| | 28.5–38.2 | 24.4–36.8 | 21.5–32.9 | 18.6–32.8 | 11.4–32.4 | 15.1–27.5 | 12.9–30.4 |
| Bin. $\Delta$-cod. $S_{bin\Delta,i}$ | | | | | | | |
| 0V% | 12.2 | 23.5 | 30.0 | 35.5 | 38.2 | 42.8 | 44.4 |
| | 9.5–22.5 | 17.6–31.2 | 25.6–35.6 | 26.2–44.9 | 30.9–48.6 | 37.1–51.8 | 29.4–57.7 |
| 1V% | 66.0 | 62.2 | 59.4 | 51.3 | 44.9 | 45.1 | 41.8 |
| | 61.7–74.4 | 56.8–69.5 | 51.6–66.4 | 46.0–65.6 | 42.4–55.2 | 38.0–50.0 | 35.0–55.6 |
| 2V% | 11.1 | 10.9 | 9.3 | 10.5 | 12.7 | 10.1 | 11.2 |
| | 8.8–23.8 | 8.2–14.4 | 5.8–16.7 | 6.6–16.1 | 4.7–17.0 | 6.5–16.6 | 6.1–15.3 |
| Bin. $\Delta$-cod. $S_{bin\Delta,10,i}$ | | | | | | | |
| 0V% | 16.0 | 27.5 | 36.8 | 42.1 | 47.2 | 54.0 | 53.3 |
| | 8.8–30.3 | 18.9–35.1 | 29.0–40.8 | 31.3–52.2 | 41.8–58.7 | 40.5–59.9 | 42.3–61.9 |
| 1V% | 62.4 | 60.3 | 50.6 | 48.2 | 41.6 | 36.4 | 35.0 |
| | 58.6–72.8 | 53.2–67.2 | 47.3–61.9 | 40.3–55.6 | 32.4–45.5 | 32.3–44.2 | 33.2–45.7 |
| 2V% | 13.8 | 12.5 | 10.9 | 10.1 | 10.7 | 9.4 | 12.1 |
| | 8.4–24.7 | 9.5–17.4 | 9.0–14.0 | 5.2–13.3 | 7.5–13.4 | 8.2–13.8 | 6.7–13.5 |

in the symbolic series $S_{\sigma,i}$ constructed using $\Delta RR_i$. On the other hand, symbolic sequences showing two unlike values are present in the symbolic series. However, $2UV\%_d$ are not affected by the different tilt angles, i.e. they are constant.

The results for the binary symbolic sequence $S_{bin\Delta,i}$ and $S_{bin\Delta,10,i}$ are as follows. For the symbolic series $S_{bin\Delta,i}$ 0V% shows a progressive increase over the whole range of tilt angles. At the same time 1V% shows a progressive decrease. 2V% is not affected by the tilt angles. For the symbolic sequences of the series $S_{bin\Delta,10,i}$ the sequences without variations (0V%) show a progressive increase up to 75°. At the same time 1V% decreases. 2V% is not affected by the tilt angle.

The results of the corresponding linear regression analysis are summarized in Table 4. The results of the global linear regression analysis correspond to the aforementioned results. For the symbolic sequence of the $\sigma$-method applied to $RR_i$ all indexes show a global linear regression. $0V\%_a$, $2LV\%_a$ and $2UV\%_a$ show a similar rate of individual linear regression (59% to 76%) whereas the rate of $1V\%_a$ is lower

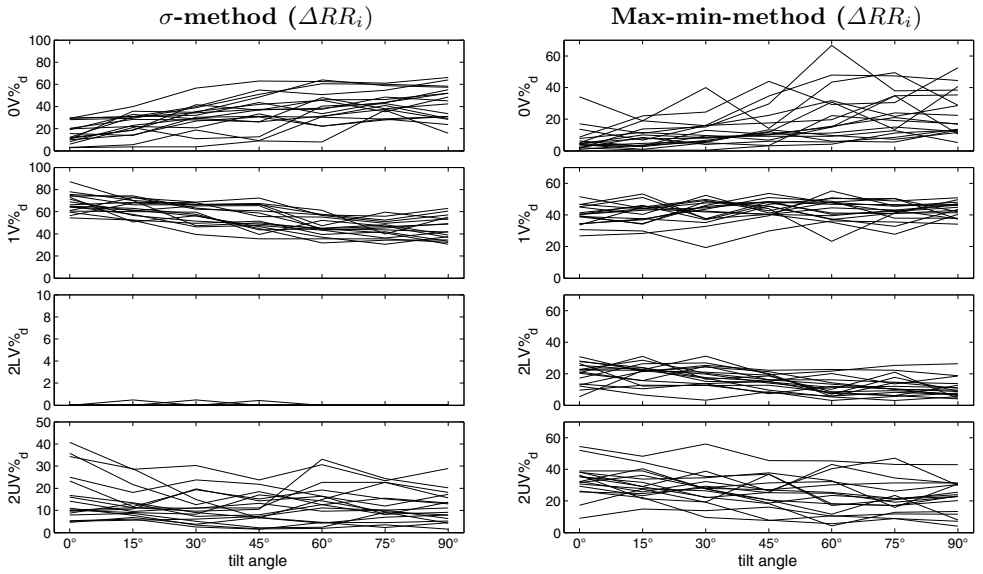


**Fig. 4.** Occurrence of symbolic sequences generated from the $\Delta RR_i$ series categorized according to the variation $0\mathrm{V}\%_d$, $1\mathrm{V}\%_d$, $2\mathrm{LV}\%_d$ and $2\mathrm{UV}\%_d$ vs. tilt angle. Left column: $\sigma$-method, right column: Max-min-method.

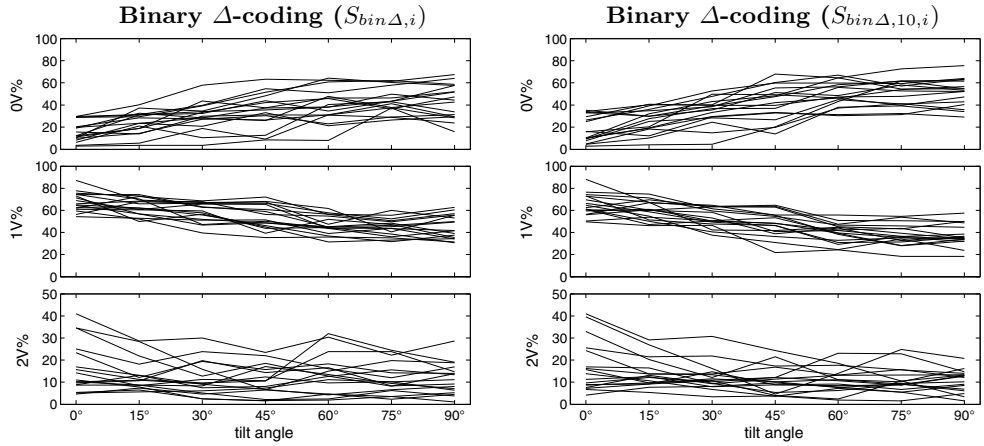


**Fig. 5.** Occurrence of binary symbolic sequences generated from the $\Delta RR_i$ series (Binary $\Delta$-coding) categorized according to the variation 0V%, 1V%,and 2V% vs. tilt angle. Left column: results of $S_{bin\Delta,i}$-series, right column: results of $S_{bin\Delta,10,i}$-series.

(35%). The symbolic sequence of the max-min-method applied to $RR_i$ shows similar results compared to the $\sigma$-method except that $1\mathrm{V}\%_a$ does not show a global linear regression and the rate of individual linear regression of $2\mathrm{LV}\%_a$ is only 41%. The $\sigma$-method applied to $\Delta RR_i$ shows slightly different results. Only $0\mathrm{V}\%_d$ and $1\mathrm{V}\%_d$ show a global linear regression but the rates of the individual linear regression is higher compared to the $\sigma$-method applied to $RR_i$ ($0\mathrm{V}\%_d$: 82%, $1\mathrm{V}\%_d$: 76%). The max-min-method applied to $\Delta RR_i$ shows a global linear regression for the same parameters than for the max-min-method applied to $RR_i$. However, the rates of the individual linear regression are different are lower for $0\mathrm{V}\%_d$ (47%) and $2\mathrm{UV}\%_d$ (47%) compared to $0\mathrm{V}\%_a$ and $2\mathrm{UV}\%_a$, respectively. For $2\mathrm{LV}\%_d$ the rate increases (47%).

**Table 4.** Results of global (GLR) and individual linear regression (ILR) analysis of symbolic indexes vs. tilt angles.

| Method | $RR_i$ | | | $\Delta RR_i$ | | |
|---|---|---|---|---|---|---|
| | Index | GLR | ILR% | Index | GLR | ILR% |
| $\sigma$-method | $0V\%_a$ | Yes | 76% | $0V\%_d$ | Yes | 82% |
| | $1V\%_a$ | Yes | 35% | $1V\%_d$ | Yes | 76% |
| | $2LV\%_a$ | Yes | 59% | $2LV\%_d$ | No | - |
| | $2UV\%_a$ | Yes | 65% | $2UV\%_d$ | No | - |
| Max-min-method | $0V\%_a$ | Yes | 76% | $0V\%_d$ | Yes | 47% |
| | $1V\%_a$ | No | - | $1V\%_d$ | No | - |
| | $2LV\%_a$ | Yes | 41% | $2LV\%_d$ | Yes | 47% |
| | $2UV\%_a$ | Yes | 65% | $2UV\%_d$ | Yes | 47% |
| Binary $\Delta$-coding ($S_{bin\Delta,i}$) | | | | 0V% | Yes | 82% |
| | | | | 1V% | Yes | 76% |
| | | | | 2V% | No | - |
| Binary $\Delta$-coding ($S_{bin\Delta,10,i}$) | | | | 0V% | Yes | 94% |
| | | | | 1V% | Yes | 88% |
| | | | | 2V% | No | - |

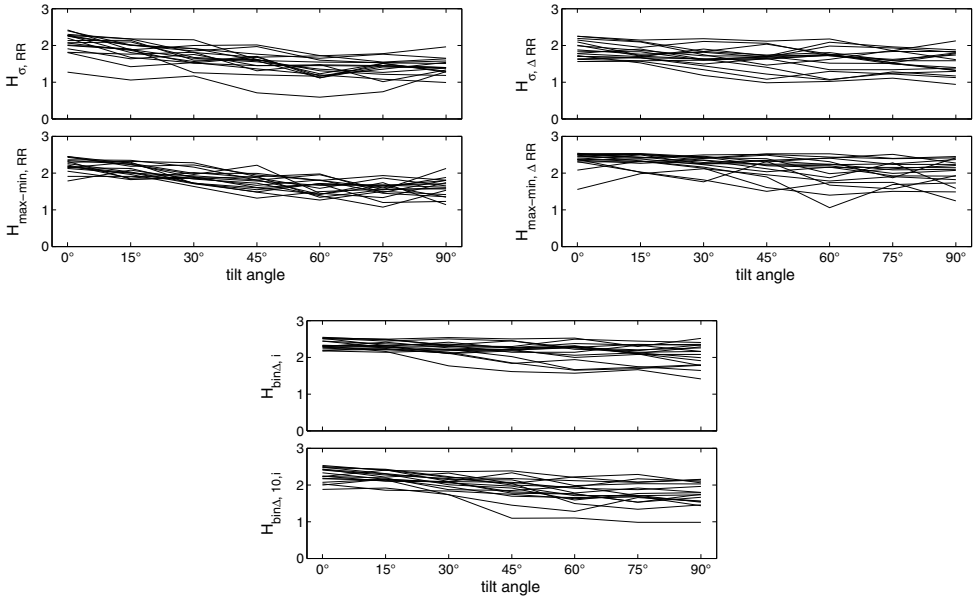


**Fig. 6.** Permutation entropy $H$ during graded head-up tilt. Top left: Entropies for the $\sigma$- and the max-min-method using $RR_i$ ($H_{\sigma,RR}$ and $H_{max-min,RR}$). Top right: Entropies for the $\sigma$- and the max-min-method using $\Delta RR_i$ ($H_{\sigma,\Delta RR}$ and $H_{max-min,\Delta RR}$). Lower diagrams show entropies for the binary $\Delta$-coding methods ($H_{bin\Delta,i}$ and $H_{bin\Delta,10,i}$).

The parameters of the binary $\Delta$-coding sequence $S_{bin\Delta,i}$ show high rates of individual linear regression: 82% for 0V% and 76% for 1V%. On the other hand 2V% does not show a linear regression at all. Using the binary $\Delta$-coding sequence $S_{bin\Delta,10,i}$ yields the highest rates of individual linear regression (0V%: 94%, 1V%: 88%).

### 3.2 Permutation entropy

Generally, the permutation entropy decreases progressively with increasing tilt angle regardless of the symbolic series used for the calculation of the entropy (see Fig. 6).

**Table 5.** Permutation entropy $H$ during graded head-up tilt calculated from the symbolic series constructed using $RR_i$ ($H_{\sigma,RR}$ and $H_{max-min,RR}$) or $\Delta RR_i$ ($H_{\sigma,\Delta RR}$ and $H_{max-min,\Delta RR}$). The entropies calculated from the binary $\Delta$-coding methods are denoted as $H_{bin\Delta,i}$ and $H_{bin\Delta,10,i}$. Values are expressed as median (1st quartile–3rd quartile).

| Index | 0° | 15° | 30° | 45° | 60° | 75° | 90° |
|---|---|---|---|---|---|---|---|
| $H_{\sigma,RR}$ | 2.13 | 1.88 | 1.67 | 1.59 | 1.35 | 1.45 | 1.39 |
| | 1.97–2.27 | 1.74–2.03 | 1.53–1.86 | 1.42–1.69 | 1.16–1.56 | 1.25–1.53 | 1.29–1.55 |
| $H_{max-min,RR}$ | 2.22 | 2.08 | 1.88 | 1.78 | 1.66 | 1.56 | 1.61 |
| | 2.14–2.34 | 1.95–2.25 | 1.73–2.00 | 1.58–1.90 | 1.42–1.80 | 1.46–1.67 | 1.39–1.80 |
| $H_{\sigma,\Delta RR}$ | 1.84 | 1.73 | 1.63 | 1.68 | 1.72 | 1.53 | 1.58 |
| | 1.70–2.10 | 1.66–1.91 | 1.57–1.84 | 1.45–1.72 | 1.32–1.77 | 1.32–1.84 | 1.31–1.80 |
| $H_{max-min,\Delta RR}$ | 2.38 | 2.38 | 2.28 | 2.24 | 2.16 | 2.08 | 2.10 |
| | 2.34–2.50 | 2.30–2.50 | 2.15–2.41 | 2.02–2.36 | 1.77–2.33 | 1.84–2.25 | 1.79–2.29 |
| $H_{bin\Delta,i}$ | 2.32 | 2.30 | 2.25 | 2.21 | 2.25 | 2.12 | 2.16 |
| | 2.26–2.50 | 2.23–2.42 | 2.13–2.34 | 2.11–2.27 | 1.98–2.30 | 1.99–2.30 | 1.79–2.33 |
| $H_{bin\Delta,10,i}$ | 2.24 | 2.19 | 2.08 | 1.96 | 1.76 | 1.71 | 1.75 |
| | 2.14–2.44 | 2.13–2.33 | 1.93–2.18 | 1.76–2.09 | 1.62–1.97 | 1.63–2.04 | 1.55–2.03 |

**Table 6.** Results of global (GLR) and individual linear regression (ILR) analysis for the different transformation methods with respect to permutation entropy vs. tilt angles.

| Method | $RR_i$ | | $\Delta RR_i$ | |
|---|---|---|---|---|
| | GLR | ILR% | GLR | ILR% |
| $\sigma$-method | Yes | 71% | Yes | 47% |
| Max-min-method | Yes | 71% | Yes | 59% |
| Bin.$\Delta$ ($S_{bin\Delta,i}$) | | | Yes | 53% |
| Bin.$\Delta$ ($S_{bin\Delta,10,i}$) | | | Yes | 82% |

Using the $\sigma$-method to transform the $RR_i$ series shows a progressive decrease of $H_{\sigma,RR}$ up to a tilt angle of 60° whereas the entropy $H_{max-min,RR}$ of the max-min-method decreases up to a tilt angle of 75° (see Table 5). For the $\sigma$-method applied to the differences $\Delta RR_i$ the results are less clear. A clear progressive decrease of $H_{\sigma,\Delta RR}$ with increasing tilt angle can only be observed up to the tilt angle of 30°. On the other hand, for the max-min-method applied to the differences $\Delta RR_i$ the permutation entropy $H_{max-min,\Delta RR}$ shows a clear progressive decrease up to 75°. The permutation entropies $H_{bin\Delta,i}$ and $H_{bin\Delta,10,i}$ calculated from the binary series $S_{bin\Delta,i}$ and $S_{bin\Delta,10,i}$, respectively, both show a progressive decrease up to the angle of 75°.

The results of the global and individual linear regression analysis resemble the aforementioned results (see Table 6). Each permutation entropy shows a global linear regression. However, the rate of individual linear regression varies between 47% and 82%. The entropies calculated from the symbolic series that was generated by the $\sigma$-method applied to $\Delta RR_i$ shows the lowest rate whereas the entropies calculated from the binary symbolic series $S_{bin\Delta,10,i}$ shows the highest rate.

## 4 Discussion

A major finding of this study is that the three presented transformations from interbeat interval series to symbolic series are capable of reflecting changes of cardiac autonomic regulation during head-up tilt. This finding is regardless of whether absolute values $RR_i$ or differences $\Delta RR_i$ were used to generate the symbolic series. Hence, symbolic indexes were linearly correlated with tilt angle. There were also linear correlations with tilt angles in a greater percentage of subjects. Furthermore,

also permutation entropy calculated from the different symbolic series can be used to quantify changes of cardiac autonomic regulation during head-up tilt. These permutation entropies also decrease linearly with tilt angle.

We speculate that the ability to typify short-term cardiovascular control might lie in the chosen pattern length (i.e. 3) and/or in the adopted procedure to group patterns into a small number of meaningful families carefully commensurate with the frame length of the series [9].

It has to be noted that the graded head-up tilt test is an experimental maneuver that activates sympathetic modulations and withdraws parasympathetic modulations [21,22]. This is reflected by the decrease of the average interbeat interval with increasing tilt angle. Using $RR_i$ for the construction of the symbolic series $0\text{V}\%_a$ increased with increasing tilt angle for both, the $\sigma$-method and the max-min-method. Hence, they reflect the increase of sympathetic modulations. On the other hand $2\text{LV}\%_a$ and $2\text{UV}\%_a$ decreased with increasing tilt angle and, hence, they reflect the decrease of parasympathetic modulations [11]. Using $\Delta RR_i$ for the construction of the symbolic series leads to similar interpretations with respect to the max-min-method. For the $\sigma$-method applied to $\Delta RR_i$ the physiological interpretation of the indices is slightly different. $0\text{V}\%_d$ reflects sympathetic modulations because it is linearly correlated to the tilt angle. Parasympathetic modulations are reflected by $1\text{V}\%_d$ because this index is negatively correlated to the tilt angle.

Two indexes of the binary analysis were also able to reflect the changes of both branches of the ANS during graded head-up tilt. For both binary series, $S_{bin\Delta,i}$ and $S_{bin\Delta,10,i}$, 0V% increases with increasing tilt angle and, hence, reflects the increase of sympathetic modulations. 1V% decreases with increasing tilt angle and reflects the decrease of parasympathetic modulations. With respect to $S_{bin\Delta,i}$ both, 0V% and 1V% account for more than 80% of all binary sequences. This result suggests that large parts of the dynamical properties are hidden in the sequence of acceleration and deceleration of the instantaneous heart rate.

It seems to be obvious by the definitions that $0\text{V}\%_a$ of both, the $\sigma$-method and the max-min-method applied to $RR_i$, reflect sympathetic modulations whereas $2\text{LV}\%_a$ and $2\text{UV}\%_a$ of both methods reflect parasympathetic modulations: sympathetic modulations are slower than parasympathetic modulations and, hence, they are captured be $0\text{V}\%_a$. In turn, faster modulations are captured by $2\text{LV}\%_a$ and $2\text{UV}\%_a$. This observation is supported by simulations of the autonomic regulation [23]. The physiological interpretation of the indexes $0\text{V}\%_d$ and $1\text{V}\%_d$ obtained by the $\sigma$-method applied to $\Delta RR_i$ is less evident. The threshold parameter $a$ (see Eq. 1) was the same regardless of whether the method was applied to $RR_i$ or $\Delta RR_i$. If applied to $\Delta RR_i$ symbolic sequences containing mostly zero or one variation are constructed (approx. 80% of the sequences are classified by the indexes $0\text{V}\%_d$ or $1\text{V}\%_d$) whereas two like variations hardly occur within symbolic sequences ($2\text{LV}\%_d$ is close to zero). Similar to the $\sigma$-method applied to $RR_i$, symbolic sequences with zero variation reflect sympathetic modulations. However, if there is one variation within the symbolic sequences the reflect parasympathetic modulations. It has to be noted that the threshold parameter $a$ could be adapted for the application to $\Delta RR_i$. However, it remains to be explored whether a different threshold results in symbolic indexes that unambiguously reflect both branches of the autonomic nervous system.

With respect to the binary sequences of length 3 obtained from the binary series $S_{bin\Delta,i}$ it is straight forward that 0V% is linked to sympathetic modulations and 1V% is linked to parasympathetic modulations regardless of the method used to construct the binary series. It has been shown for binary sequences of length 8 that binary sequences with a low number of variations (i.e. acceleration or deceleration of the heart rate lasting a few heartbeats) reflect sympathetic modulations whereas some binary patterns with a high number of variations (i.e. more complex sequences) are linked to

parasympathetic modulations [16]. The present result suggest that these relationships hold even for binary sequences of length 3. The binary series $S_{bin\Delta,10,i}$ also reflects sympathetic (0V%) and parasympathetic modulations (1V%). It has to be explored whether successions of 0s or 1s (or both) contribute to 0V% in order to elucidate the physiological interpretation of the symbolic indexes.

The permutation entropy is also able to reflect physiological changes of cardiac autonomic control during graded head-up tilt. It reflects parasympathetic modulations because the entropy decreases with increasing tilt angle regardless of the method to construct the symbolic series. The results show that the application of permutation entropy has the potential to be interpreted in terms of physiological functioning. It remains to be shown if more detailed information can be obtained if the ordinal patterns are analyzed supplementing the information of permutation entropy.

It remains to be explored whether the relationship between symbolic indexes and modulations of the ANS could be related to some intrinsic characteristics of symbolic analysis, such as the interpretation of nonlinear components, to the elimination of conventional definition of frequency bands, or to the specific pattern decomposition scheme exploited by this analysis or strategies to group patterns into a small number of classes. Furthermore, the impact of the definition of the transformation has to be explored in more detail. For the $\sigma$-method e.g. the definition of threshold as relative deviations from the average $RR_i$ ($\pm 5\%$) could have an impact because if the average $RR_i$ is 1000 ms the thresholds are 1000 ms $\pm$ 50 ms whereas if the average $RR_i$ is lower also the threshold are closer to the average (e.g. 800 ms $\pm$ 40 ms). This definition could be replaced by a static definition of the threshold (e.g. $avg(RR_i) \pm 50$ ms). For the Max-min-method the quantization levels are calculated for each time series. To achieve relative consistency between different time series it may be useful to use a global definition of the quantization levels (using e.g. the global maximum, the global minimum and $\xi$ quantization levels).

## References


1. M. Malik, et al., Circulation **93**, 1043 (1996)
2. G.G. Berntson, et al., Psychophysiology **34**, 623 (1997)
3. S. Akselrod, et al., Science **213**, 220 (1981)
4. J. Kurths, et al., Chaos **5**, 88 (1996)
5. N. Wessel, et al., Int. J. Bifurcat. Chaos. **17**, 3325 (2007)
6. A. Voss, et al., Cardiovasc. Res. **31**, 419 (1996)
7. A. Suhrbier, et al., Chaos **20**, 045124 (2010)
8. M.M. Kabir, et al., Ann. Biomed. Eng. **39**, 2604 (2011)
9. A. Porta, et al., IEEE Trans Biomed. Eng. **48**, 1282 (2001)
10. S. Guzzetti, et al., Circulation **112**, 465 (2005)
11. A. Porta, et al., Am. J. Physiol. Heart Circ. Physiol. **293**, H702 (2007)
12. D. Cysarz, et al., Am. J. Physiol. Heart. Circ. Physiol. **278**, H2163 (2000)
13. J.W. Kantelhardt, et al., Phys. Rev. E **65**, 051908 (2002)
14. D. Cysarz, et al., Am. J. Physiol. Regul. Integr. Comp. Physiol. **292**, R368 (2007)
15. C. Cammarota, E. Rogora, Phys. Rev. E **74**, 042903 (2006)
16. D. Cysarz, et al., Comp. Biol. Med. **42**, 313 (2012)
17. P. Guzik, et al., J. Electrocardiol **45** 70 (2012)
18. U. Meyerfeldt, et al., Int. J. Cardio. **84**, 141 (2002)
19. R. Huhle, et al., Physiol. Meas. **33**, 207 (2012)
20. C. Bandt, B. Pompe, Phys. Rev. Lett. **88**, 174102 (2002)
21. W.H. Cooke, et al., J. Physiol. **517**, 617 (1999)
22. R. Furlan, et al., Circulation **101**, 886 (2000)
23. E. Tobaldini, et al., IEEE Eng. Med. Biol. Mag. **28**, 79 (2009)